Biomedicine and Chemical Sciences 2(2) (2023) 76-82

2-BCS-2017-456

Content lists available at:
www.journals.irapa.org/index.php/BCS/issue/view/23

Biomedicine and Chemical Sciences

Journal homepage: https://www.journals.irapa.org/index.php/BCS

The Role of Gold Nanoparticles/Au-PEG-PAMAM as Drug Delivery System for Treatment of Breast Cancer

Murtadha M-Hussein A-Kadhim[1] & Ali Hamad Abd Kelkawi[2*]

[1] *Department of Genetic Engineering, College of Biotechnology, AL-Qasim Green University, Ministry of Higher Education and Scientific Research – Iraq*
[2] *Department of Medical Physics, College of Applied Medical Sciences, University of Kerbala, Ministry of Higher Education and Scientific Research – Iraq*

ARTICLEINFO

Article history:
Received on: February 02, 2023
Revised on: March 15, 2023
Accepted on: March 20, 2023
Published on: April 01, 2023

Keywords:
AuNPs
Au-PEG-PAMAM-DOX
Drug Delivery
Synthesis technique

ABSTRACT

To enhance the cellular uptake and chemotherapeutic efficacy of a current chemotherapeutic medication, a nanoparticle drug carrier technology has been designed. Due to their distinctive electrical and optical characteristics, gold nanoparticles (Au NPs) have recently demonstrated intriguing medical and military uses. In the event that they come into touch with a biological system, little is known about their biocompatibility. Metallic nanoparticles have been successfully utilized for a kind of biological applications. A drug delivery system known as Au – PEG – PAMAM – DOX was produced by conjugating the dendrimer with the anti-cancer chemical doxorubicin (DOX) via an amide bond. The amount of DOX released from Au – PEG – PAMAM – DOX at a natural pH was negligible, but this amount significantly increased in an environment with a weak acidic milieu, according to studies on the release of medicines from acellular sources. A research into the intracellular release of the medication was carried out with the assistance of confocal laser scanning microscopy (CLSM). Recently conjugation to the nanosystem, in vitro viability experiments revealed an increase in the associated DOX cytotoxicity that could not be attributable to carrier components. This indicates that the effectiveness of the DOX was increased. In light of this, it has been hypothesized that the newly created pH-triggered multifunctional Au NPs- DOX nanoparticle system could pave the way for a viable platform for the intracellular delivery of a range of anticancer medicines. In the current study, the common Au NPs synthesis techniques and their well-established uses in diverse needs, particularly in biological sensing applications.

1. Introduction

Cancer is one of the world's major causes of death. According to the American Cancer Society, there will be 1,7 million newly diagnosed cancer cases in 2018, with over a third of these cancer patients dying, with breast cancer playing a key role in these numbers (Siegel, et al., 2018). Ionizing radiation, together with chemotherapy and surgery, is used as part of a comprehensive cancer treatment in more than half of cancer patients (Atun, et al., 2015). Unfortunately, for many types of cancer, radiation therapy is only effective at large doses, and this strategy frequently results in toxicity to surrounding normal tissue, causing early and late side effects that can decrease patients' quality of life (Rosa, et al., 2017). Radiation-induced cytotoxicity has been a major limiting factor in optimizing deposited radiation doses to cancer tissues since it was first recognized in the late nineteenth century, and as such has been a substantial impediment in cancer treatment planning (Bentzen, 2006). In this study, we designed a gold nanoparticle-based drug delivery nanosystem to modify the intracellular drug release of DOX in vitro by means of an enhanced permeability and retention (EPR) effect.

Owing to their biocompatibility and unique optical, physical, and electrical properties, gold nanoparticles are widely employed in biomedical nanotechnologies for targeted drug delivery (Tian, et al., 2014; Dreaden, et al., 2012). Due to the surface plasmon resonance features of the Au NPs, it has also been reported that the intracellular drug delivery

***Corresponding author:** Murtadha M-Hussein A-Kadhi, Department of Genetic Engineering, College of Biotechnology, AL-Qasim Green University, Ministry of Higher Education and Scientific Research – Iraq

E-mail: **murbt@biotech.uoqasim.edu.iq**

How to cite:

A-Kadhim, M. M.-H., & Kelkawi, A. H. A. (2023). The Role of Gold Nanoparticles/Au-PEG-PAMAM as Drug Delivery System for Treatment of Breast Cancer. *Biomedicine and Chemical Sciences, 2*(2), 76–82.

DOI: **https://doi.org/10.48112/bcs.v2i2.456**

location can be monitored utilizing 4 surface enhanced Raman scattering (SERS) (Liu, et al., 2016; Zong, et al., 2013). Au nanoparticles are frequently treated with polymers such as poly (ethylene glycol) (PEG) to increase its stability without affecting its biocompatibility, while simultaneously enhancing its potential for biomedical applications (Lee, et al., 2015; Zhong, et al., 2014). In general, the inclusion of the PEG polymer is known to increase the electrostatic repulsion between nanoparticles, hence enhancing the stability of colloidal Au NPs (Moustaoui, et al., 2016).

It has also been demonstrated that the coupling of a PEG polymer to Au nanoparticles increases it is accumulation at tumor locations in vivo by increasing the nanoparticles' circulation duration (Gao, et al., 2012). Hence, PEG conjugation on the surface of spherical Au nanoparticles may assist minimize deleterious effects and reduce their uptake by the reticuloendothelial system (RES) during circulation in the bloodstream (Lazarovits, et al., 2015; Jokerst, et al., 2011). The overall efficacy of drug delivery systems is dependent on the drug loading capacity of nanoparticles. Dendrimers are useful for the simultaneous conjugation of drugs and targeting ligands, and their structures have the potential to increase the drug loading capacity owing to their highly branched nature, 3-D spherical morphology, surface multi-functionality, and well-defined composition (Lane, et al., 2015; Bugno, et al., 2015).

We report a unique pH-responsive PEGylated dendrimer modified drug coupled Au NPs as a smart drug delivery system for chemotherapeutic purposes. Currently, data on the combined use of a PEG polymer and poly amido amide (PAMAM) dendrimers with doxorubicin for cancer therapy are rare in the scientific literature, and there in vitro interactions are explored in scant detail (Kurniasih, et al., 2015; Zhang, et al., 2011). Huang et al. used confocal laser scanning microscopy (CLSM) to study the intracellular activity of nanoparticles in order to create nanoparticle-based drug delivery devices (He, et al., 2011; Huang, et al., 2013). Li et al. (2014) described photothermal-chemotherapy employing a drug delivery system including 5 PEGylated dendrimer-doxorubicin attached gold nanorods. This system requires a linker to conjugate doxorubicin in five steps; however, in the present investigation, the nanosystem was synthesized in four steps employing a modified PEG as a stabilizing agent instead of a linker. This study describes the fabrication of the drug delivery vehicle Au-PEG-PAMAM-DOX conjugate and the tracking of intracellular drug release using confocal laser scanning microscopy (CLSM) images.

2. Materials and Methods

Materials and Chemicals

Trisodium citrate dehydrate, 1-ethyl-3-(3-dimethylaminopropyl) carbodimide hydrochloride, N-hydroxysulfosuccinimide, and gold(III) chloride trihydrate (HAuCl4.3H2O) (NHS) were purchased from Santa Cruz Biotechnology. PAMAM dendrimer succinamic acid 10% in water solution was purchased from Sigma, diisopropyl ethylamine (DIPEA) and doxorubicin hydrochloride (DOX) were purchased from Santa Cruz Biotechnology, Cell culture media Dulbecco's Modified Eagle Medium (DMEM), all supplements, Fetal Bovine Serum (FBS), L-Glutamine, Streptomycin, trypsin from Sigma.

Preparation of Au NPs

In a brief, a solution containing 1 mM $HAuCl4.3H2O$ was brought to a boil in 100 ml of water while being rapidly agitated throughout the process. Following this, 10 ml of 40.0 mM sodium citrate was added to the mixture. As a result, the solution's color changed from light yellow to deep red. After 10 minutes of continuous boiling, the heating was turned off, and the solution was agitated for a further 15 minutes (Tian, et al., 2014). The created nanoparticles were kept in a freezer at 4 °C. until needed.

Loading of PEG thiol with Au NPs

In order to functionalize the Au NPs, 1 mM of SHPEG-NH2 (MW 5 kDa) was added to a 30 µM of 70 ml Au NPs solution, and the mixture was agitated for an additional 15 minutes. The mixture was then left to react at 4 °C. overnight (Dreaden, et al., 2012). After that, the unreacted PEG was separated from the solution by employing a dialysis membrane with a MWCO of 30 kDa. The sample was then washed three times with ultrapure water, and the purified product was stored at a temperature of 4 °C.

Au-PEG modification using a PAMAM

A water solution of PAMAM-COOH (2 ml containing 2 mg), EDC.HCl (1.78 mg), and NHS (1 mg) was added to the Au-PEG NPs in order to cause a change in their structure. In order to activate the carboxylic group of PAMAM, the mixture was agitated for a period of thirty minutes while the temperature was maintained at room temperature. The Au-PEG NPs solution (50 ml, 14 µM AuNPs conc.) was agitated for an additional 48 hours after the addition of this solution (Liu, et al., 2016; Zong, et al., 2013). The solution was then dialyzed one more time using a dialysis membrane (MWCO 30 kDa) and the temperature was maintained at 4 °C in order to eliminate any unreacted PAMAM.

Conjugation of $Au - PEG - PAMAM\ NPs$ with doxorubicin hydrochloride (DOX)

After mixing the produced Au-PEG-PAMAM NPs (30 ml) at 0 °C for five minutes, the following steps were carried out: the addition of HBTU (3.5 mg) and DIPEA (4.31µl) was followed by an additional ten minutes of stirring. A solution of doxorubicin (1 ml containing 2 mg) was then added to the mixture, and the reaction was stirred for forty-eight hours at room temperature without being exposed to light from the outside (Lee, et al., 2015). The completed product was then dialyzed once more over a dialysis membrane with a MWCO of 30 kDa to eliminate any remaining free DOX before being stored at 4 °C.

Drug loading efficiency

The drug loading efficiency was estimated using a direct method based on the absorption of the DOX at 480 nm. In brief, the nano-carrier system's unknown drug concentration was calculated using a calibration curve based on a series of known DOX values. The drug loading efficiency was then determined using the equation (1)

$$\text{Loading efficiency \%} = \frac{\text{Amount of drug in micelle}}{\text{Total amount of drug in feed}} \times 100\% \quad \ldots. \ (1)$$

Physicochemical characterization of drug delivery system

Using a SpectraMax M3 multi-mode microplate reader, absorption measurements at 480 nm and fluorescence measurements at 471 nm were performed (Molecular Devices, USA). Using the Zetasizer nano analyzer, the hydrodynamic size, polydispersity index (PDI), and zeta potentials of the nanoparticles were determined (Malvern Instruments, Worcestershire, UK). The Hitachi SU 6600 FESEM apparatus was used for scanning electron microscopy (SEM) analysis. The SEM samples were created by spinning a nanoparticle solution at 1000 rpm for 20 seconds on prewashed silicon substrates and drying them in air in a dust-free environment. Transmission electron microscopy (TEM) investigation was performed on an FEI Tecani F30 with a 300 kV accelerating voltage. A drop of sample was placed on a coated 400 mesh Copper grid and evaporated in air at room temperature to produce the TEM images. In TEM mode, the point resolution is 0.19 nm. Confocal pictures were captured using a Zeiss 510 laser scanning microscope (Oberkochen, Germany).

Cell culture

The MCF7 cell line (human breast cancer) was obtained from Santa Cruz and grown in DMEM media supplemented with 10% FBS, 45 IUml-1 penicillin, and 45 IUml-1 streptomycin in a humidified 5% CO2 incubator at 37 °C.

3. Results and Discussion

Synthesis and characterization of $Au-PEG-PAMAM-DOX$

As mentioned earlier, we generated a pH-sensitive $Au-PEG-PAMAM-DOX$ The purpose of this nano system is to modify the cellular absorption process and enhance the efficacy of DOX treatment at acidic cancer locations. A PEGylated Au sphere PAMAM polymeric conjugate was synthesized using a manufacturing method that included multiple stages. By reducing gold chloride with citrate, Au NPs were made. CN, NH_2, and SH are all examples of polymer functional groups that can be employed to stabilize Au through the formation of covalent bonds. These groups are extremely attractive to Au NPs. In order to further improve the citrate-capped Au'NPs resistance to hydrolysis, a thiolated PEG polymer was later applied to their surface. The biocompatibility of nanoparticles can be improved by coating the surface of the particles with dendrimer molecules. Following the application of PEG for stabilization, the surface of the Au NPs was modified with a carboxylated PAMAM polymeric matrix using an EDC coupling process. This procedure involved the formation of an amide bond between the dendrimer and the amine group of the PEG polymer. In the final step, an amide bond was formed between the DOX and the carboxylic acid group of the PAMAM by employing DIPEA as a base and HBTU as a coupling agent. This step was necessary for the production of the final $Au-PEG-PAMAM-DOX$ carrier system. In order to confirm the effective conjugation of $PEG-SH,G4-PAMAM$ dendrimer to Au NPs and drug loading on the nanosystem, a comprehensive characterization of the nanosystem $Au-PEG-PAMAM-DOX$ was performed utilizing UV-Vis absorption spectra. In Figure 1A, The UV-Vis absorption spectra of Au NPs, Au-PEG, Au-PEG-PAMAM, and Au-PEG-PAMAM-DOX are all displayed here for your viewing pleasure. It is standard practice to attribute the red shift in the absorbance peak of Au NPs to a slight change in the refractive index of the local surrounds of Au NPs. This change reveals itself as a red shift in the absorbance spectrum. It has been seen that the absorbance spectrum has shifted in this way (Li, et al., 2014). Conjugation of PEG, PAMAM, and DOX onto the surface of Au NPs resulted in a green shift of the longitudinal surface plasmon resonance band of 3 nm, 2 nm, and 2 nm, respectively, as can be seen in Figure 1A. This shift can be attributed to the fact that PEG, PAMAM, and DOX are all conjugated onto the surface of Au NPs. PEG, PAMAM, and DOX were successfully conjugated onto the surface of the Au NPs, as evidenced by the differences in the absorbance spectra of the Au NPs, which were regarded as proof. When the 480 nm absorption peak of the DOX in $Au-PEGPAMAM-DOX$ was compared to a standard curve using absorption spectroscopy, the average loading efficiency was found to be 45.85% (an average of n = 3 batches) of the DOX that was present in total in the nano-carrier solution. This was determined by taking the average of the results from all three batches. Figure 1b demonstrates this, as may be viewed here.

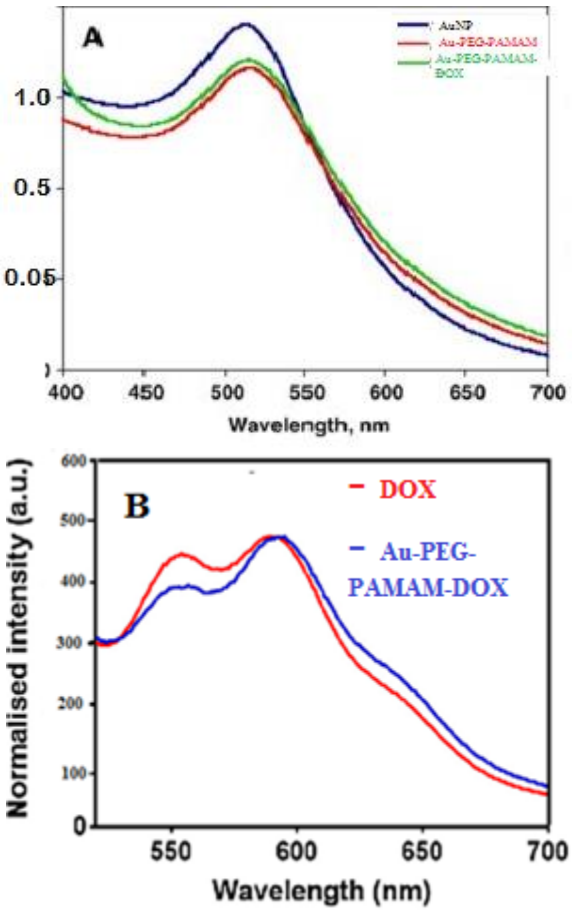

Fig. 1. (A). demonstrates the ultraviolet and visible absorption spectra of the Au-PEG-PAMAM-DOX Nano system as well as its intermediate product. (B) the fluorescence spectra of DOX and the Au -PEG-PAMAM-DOX Nano system.

In addition, fluorescence spectroscopy was used to characterize the DOX-loaded Nano carriers as well as the DOX solution, and the results were compared to an equivalent DOX concentration of 10 g/ml. The fluorescence of the $Au-PEG-PAMAM-DOX$ nano-system revealed the expected emission band from the DOX, albeit at a reduced intensity when compared to the fluorescence spectra of a free DOX solution (normalised by 1.50 multiplication). This lessening in the fluorescence emission intensity of the bound DOX would also lend support to the DOX's effective conjugation to the PAMAM. The red shift that can be detected in the absorbance spectrum can also be seen in the emission spectra of nanocarriers that have been loaded with DOX, as can be seen in Figure 5B. On the other hand, there is a fall in intensity in the region with lower wavelengths, while there is an increase in intensity in the region with higher wavelengths.

These declines may be the result of aggregation of the nanosystem (self-absorption effect), nevertheless, are more likely to be caused by the conjugation of the DOX to the PAMAM, which dampens the emission of the DOX (Venkatesan, et al., 2013). This, in conjunction with the results of the absorption spectroscopy, demonstrates that the DOX molecules were able to successfully bind with the surface of the Au NPs, hence verifying the development of the DOX-loaded nanocarrier. The zeta potential measurement of the sample provided additional proof that the nanocarrier was successfully formed; the values of the zeta potential that were obtained for the Au-PEG-PAMAM-DOX nanosystem at various phases of production are displayed. The zeta potential of Au-PEG, which had an average value of 15.0, 0.9 mV before conjugation with Au Nanoparticles, became more positive after the conjugation process (average value -35.43 1.5 mV). The negative charge carried by the gold nanoparticles is shielded and neutralized by the charge-neutral PEG (Ganta, et al., 2008). When Au NPs are coupled with more neutral PEG, the resulting Au-PEG nanoparticle has a positive charge. This is because the negative charge of the Au NPs is converted into a positive charge by the connection. The surface zeta potential changed to an average value of -14.47 1.32 after the functionalization of Au-PEG with negatively charged PAMAM G4 dendrimer.

This indicates that the carboxylic groups of the PAMAM dendrimer were covalently conjugated with the amino groups of the Au-PEG via an EDC coupling reaction. The surface zeta potential changed to this value after the functionalization of Au-PEG with negatively charged PAMAM G4 dendrimer. The variation in surface zeta potential was measured, which allowed this conclusion to be drawn. It is possible that the DOX medicine was successfully loaded onto the surface of Au-PEG-PAMAM nanoparticles due to the fact that the conjugation of positively charged doxorubicin resulted in changes in the surface zeta potential of Au-PEG-PAMAMG4-DOX (with an average value of -9.69 1.30). TEM and SEM were utilized in order to measure the particle size of the Au-PEG-PAMAM-DOX nanosystem. Micrographs taken using TEM and SEM of the nano. Revealed that the nanoparticles' sizes ranged from 15 nm to 20 nm as showed Figure 2.A. The hydrodynamic diameters of each nanoparticle were measured using a technique called dynamic light scattering (DLS). According to the information that is presented, the diameter of each and every nanoparticle measured less than 100 nm on average Figure 2.B, and the values of their PDI spanned the range of 0.5 to 0.7. It has been established that nanoparticles with an average particle size of less than 100 nm are more effective for the goal of passively targeting tumors (Ganta, et al., 2008).

There had been no instances of agglomeration at any time during the course of the synthesis; rather, there had been a progressive rise in particle size as a result of the conjugation of PEG and the dendrimer to the system. This had led to the gradual increase in particle size. As can be observed in Figure 5, the absorption band of the nanoparticles did not show any signs of broadening while the experiment was being carried out. When Au NPs were treated with PEG conjugation, an intermolecular hydrogen bond was formed between the water molecule and the conjugated PEG molecule (Zhang, et al., 2010). This prevented the gold nanoparticles from aggregating into larger clusters. The hydrophilicity of the treated Au NPs was able to be increased, which allowed this goal to be achieved. Dendrimers were incorporated into the formulation so that they could assist in the stability of the nanoparticles and prevent agglomeration (Iacovita, et al., 2015). The Nano system $AuNPs-PEG-PAMAM-DOX$ was totally dispersed in water, and it did not exhibit any evidence of agglomeration. This was corroborated by the system's persistent dispensability, which indicated that there was no aggregation. The TEM and SEM clearly demonstrated this point.

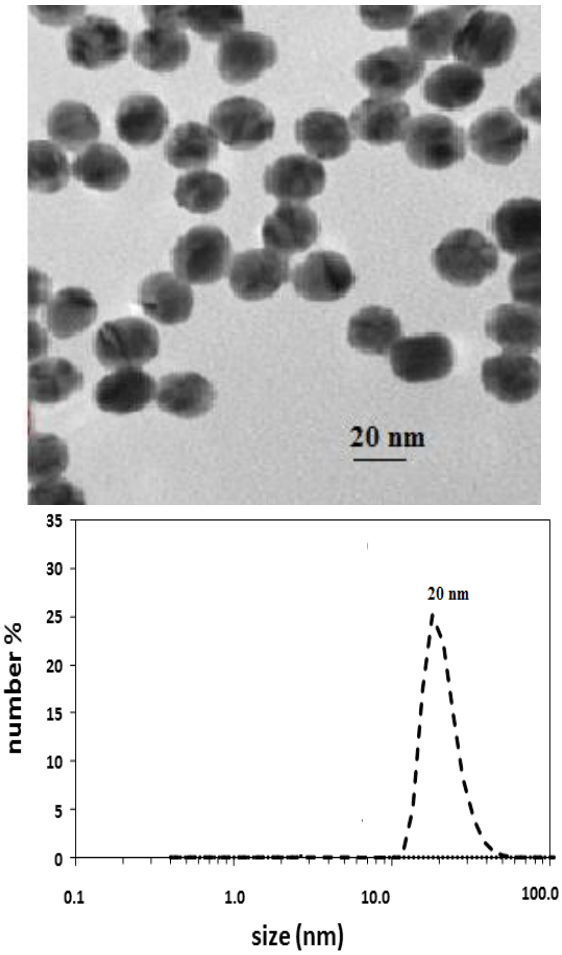

Fig. 2. A. TEM images of Au nanoparticles of averaged diameter 20 nm, B) DLS spectra showing particle sizes of 20 nm.

Acellular DOX release

Because controlling the release of the payload (drug) is the ultimate objective of any nanocarrier, the kinetics of the drug delivery system based on $Au-PEG-PAMAM-DOX$ were studied through the use of a dialysis technique. In order to simulate cellular lysosomal compartments in vitro, the nanosystem was incubated in a buffer solution with a physiological pH (pH 7.0). Additionally, the nanosystem was treated in an acidic buffer solution (pH 4.0). The time-dependent DOX release curves of $Au-PEG-PAMAM-DOX$ at pH 7.0 and pH 4.0 are depicted in Figure 2. There was no discernible DOX leakage from the $Au-PEG-PAMAM-DOX$ compound when the pH was 7.0. In contrast, we found that after 96 hours at a pH of 4.0, there was roughly a 50% release of DOX from the Nano system. We suspect that this was caused by the amide bond cleavage that occurred between the DOX and the dendrimer. The data release profile demonstrated that nanoparticles released more drug than conventional particles, and, more crucially, that the drug was released in a regulated way over a period of 96 hours at a pH of 4.0.

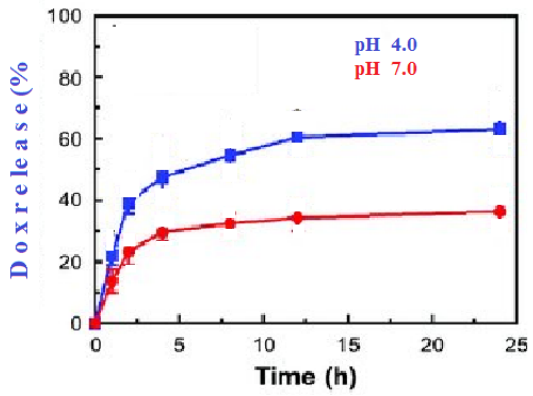

Fig. 3. pH dependent release of DOX by in Au-PEG-PAMAM-DOX Nano system.

When measured against a healthy pH of 7.0, the system that was built reveals a substantial amount of untapped potential for further development in specific applications. In order to gain a deeper comprehension of the drug release kinetics, the data on drug release were analyzed using a zero order kinetics model at a pH of 4. The zero order model is more useful for slow drug release kinetics (Crooks, et al., 2001). The equation (2) was used to display the release data against time and assess the release kinetics:

$Qt = Q0 + K0t$ Eq. 2 .... (2)

Cell viability

The MTT assay was utilized to determine the level of cytotoxicity exhibited in vitro by free DOX, Au-PEG-PAMAM and Au-PEG-PAMAM-DOX. When developing the nanosystem, the components of the $Au-PEG-PAMAM-DOX$ system were employed as a point of reference in order to establish whether or not the entire system was more effective than the free DOX. A total of 48 hours was spent to the MCF7 cells to each drug at doses ranging from 1.25 g/ml all the way up to 10 g/ml (or DOX equivalent Au concentration). As can be shown in Figure 7, $Au-PEG-PAMAM-DOX$, free DOX, Au NPs, and $Au-PEG-PAMAM$ all displayed dose- and time-dependent cytotoxicity profiles.

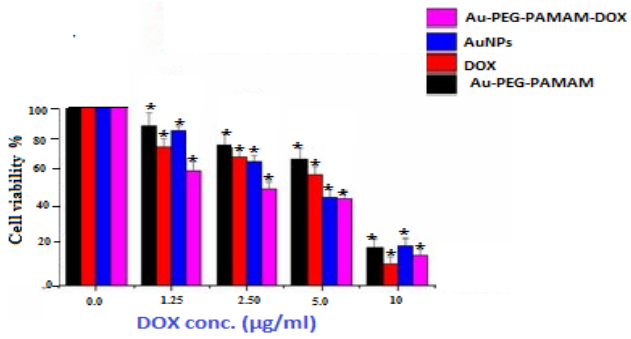

Fig. 4. In vitro cytotoxicity of MCF7 cells treated with different concentrations of Au- PEG-PAMAM-DOX, free DOX, Au and Au-PEG-PAMAM materials after 48h the process of incubation Data is presented as a percentage of the control mean with a standard deviation taken from three separate trials. A statistically significant difference from the unexposed control is indicated by a value of $P < 0.05$.

It was found that the conjugated PAMAM dendrimer on the surface of the Au PEG-PAMAM material was the source of the material's statistically significant loss in viability while having a minor impact on cell viability (Golshan, et al., 2017; Gürbüz, et al., 2016). The finding that an increase in exposure duration had a negative effect on cell viability was supported by this finding. It is important to notice that the $Au-PEG-PAMAM-DOX$ nanoparticles showed a higher level of cytotoxicity compared to free DOX, Au NPs, and $Au-PEG-PAMAM$ nanoparticles. This finding suggests that the final system boosts the effectiveness of the DOX. In comparison, the free DOX produced an IC50 of 0.40 ng/ml while the $Au-PEG-PAMAM-DOX$ produced an IC50 of 0.31 g/ml after being exposed for 48 hours. For $Au-PEG-PAMAM$, the IC50 was 15 ng/ml. Even though the differences in viability levels were not as noticeable after longer exposures, the results indicate that the development of the Nano carrier system could dramatically modify the rate at which the DOX kills the cell. This is evidenced by the differing IC50 values in the less than 48-hour exposures.

In vitro confocal imaging

As can be seen in Figure 8, the procedure of monitoring drug release and accumulation in vitro was completed with the assistance of CLSM and counterstaining the nuclei of MCF7 cells. This was done so that the results could be analyzed. Following the DOX emission made it possible to observe not just where the DOX was accumulating but also where it was being produced. PEGylated dendrimer nanoparticles have been shown to be internalized into cells by an EPR effect and to reside outside of the nucleus, most likely in the lysosomal compartments of the cell (Wolinsky & Grinstaff, 2008). This was discovered through a series of experiments in which the nanoparticles were subjected to magnetic fields. As can be seen in Figure 8, following a four-hours incubation with the $Au-PEG-PAMAM-DOX$ Nano system, the drug had collected in the lysosomal

compartment of the cells, as shown by the red fluorescence emitted by DOX. This was observed. These findings lend credence to the hypothesis that we have developed a pH-sensitive release system for DOX. This hypothesis is also supported by the results of the investigation into the acellular release of DOX, which demonstrated that the medication was liberated from the nanosystem when the pH was adjusted to 4.0. (Fig. 5). As illustrated in Figure 8, the red fluorescence emitted by DOX could be observed in both the cytoplasm and the cell nucleus after the incubation period was prolonged to a total of 24-hours. It first went into the cytoplasm, where it accumulated in the lysosomes; then, after a period of 24 hours, there was a release of the drug from the lysosomes, and it went into the nucleus of the cell. These data demonstrate beyond a reasonable question that the Au-PEG-PAMAM-DOX Nano system did, in fact, release the DOX in a controlled manner.

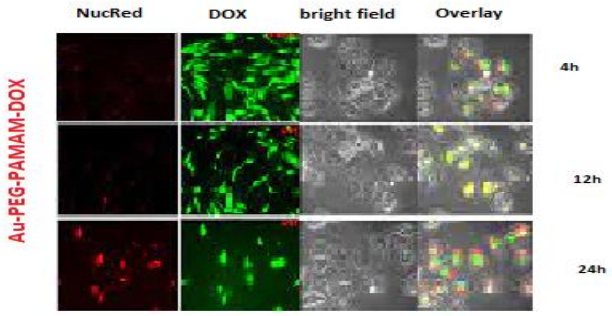

Fig. 5. Employing an Au-PEG-PAMAM-DOX nanosystem, Materials were fixed with formalin, washed, and treated with MCF7 cells for 4, 12, and 24 hours before CLSM observation. The green fluorescence is related with Nuc Red with 24 excitations at 633 nm, Emmission at 649-799 nm.

4. Conclusion

Nanosystem comprised of DOX and Au NPs ($Au-PEG-PAMAM-DOX$). In comparison to the citrate polymer coated Au, the PEG polymer coated Au NPs displayed increased levels of colloidal stability and surface area. minimal levels of toxicity while maintaining biocompatibility. The active ingredient DOX was conjugated onto the completed system with the assistance of a dendrimer and an amide bond. Because the nanocarrier was shown to enter the cell via a distinct mechanism and accumulate in the lysosomal compartments (pH 4-5) of the cells, the pH-sensitive drug release that was demonstrated by the final drug delivery system $Au-PEG-PAMAM-DOX$ was later confirmed in in vitro tests. This was done because the pH-sensitive drug release was demonstrated by the final drug delivery system. The Au-PEG-PAMAM-DOX Nanoparticle, which had DOX loaded onto it, caused a shift in the manner in which DOX was taken up by cells. This, in turn, had an effect on the cytotoxicity that was associated with DOX and improved the DOX's effectiveness when used in short-term exposures. The $(Au-PEGPAMAM-DOX)$ nanosystem is an unique multifunctional dendrimer-based nanosystem that may offer a new platform for the intracellular release of anticancer drugs at tumor locations.

Competing Interests

The authors have declared that no competing interests exist.

References

Atun, R., Jaffray, D. A., Barton, M. B., Bray, F., Baumann, M., Vikram, B., ... & Gospodarowicz, M. (2015). Expanding global access to radiotherapy. The Lancet Oncology, 16(10), 1153-1186. **https://doi.org/10.1016/S1470-2045(15)00222-3**

Bentzen, S. M. (2006). Preventing or reducing late side effects of radiation therapy: radiobiology meets molecular pathology. Nature Reviews Cancer, 6(9), 702-713. **https://doi.org/10.1038/nrc1950**

Bugno, J., Hsu, H. J., & Hong, S. (2015). Recent advances in targeted drug delivery approaches using dendritic polymers. Biomaterials science, 3(7), 1025-1034. **https://doi.org/10.1039/C4BM00351A**

Crooks, R. M., Zhao, M., Sun, L., Chechik, V., & Yeung, L. K. (2001). Dendrimer-encapsulated metal nanoparticles: synthesis, characterization, and applications to catalysis. Accounts of chemical research, 34(3), 181-190. **https://doi.org/10.1021/ar000110a**

Dreaden, E. C., Austin, L. A., Mackey, M. A., & El-Sayed, M. A. (2012). Size matters: gold nanoparticles in targeted cancer drug delivery. Therapeutic delivery, 3(4), 457-478. **https://doi.org/10.4155/tde.12.21**

Ganta, S., Devalapally, H., Shahiwala, A., & Amiji, M. (2008). A review of stimuli-responsive nanocarriers for drug and gene delivery. Journal of controlled release, 126(3), 187-204. **https://doi.org/10.1016/j.jconrel.2007.12.017**

Gao, J., Huang, X., Liu, H., Zan, F., & Ren, J. (2012). Colloidal stability of gold nanoparticles modified with thiol compounds: bioconjugation and application in cancer cell imaging. Langmuir, 28(9), 4464-4471. **https://doi.org/10.1021/la204289k**

Golshan, M., Salami-Kalajahi, M., Roghani-Mamaqani, H., & Mohammadi, M. (2017). Poly (propylene imine) dendrimer-grafted nanocrystalline cellulose: Doxorubicin loading and release behavior. Polymer, 117, 287-294. **https://doi.org/10.1016/j.polymer.2017.04.047**

Gürbüz, M. U., Öztürk, K., Ertürk, A. S., Yoyen-Ermis, D., Esendagli, G., Çalış, S., & Tülü, M. (2016). Cytotoxicity and biodistribution studies on PEGylated EDA and PEG cored PAMAM dendrimers. Journal of Biomaterials science, Polymer edition, 27(16), 1645-1658. **https://doi.org/10.1080/09205063.2016.1226044**

He, H., Li, Y., Jia, X. R., Du, J., Ying, X., Lu, W. L., ... & Wei, Y. (2011). PEGylated Poly (amidoamine) dendrimer-based dual-targeting carrier for treating brain tumors. Biomaterials, 32(2), 478-487. **https://doi.org/10.1016/j.biomaterials.2010.09.002**

Huang, F., Watson, E., Dempsey, C., & Suh, J. (2013). Real-time particle tracking for studying intracellular trafficking of pharmaceutical nanocarriers. Cellular and

Subcellular Nanotechnology: Methods and Protocols, 211-223. https://doi.org/10.1007/978-1-62703-336-7_20

Iacovita, C., Stiufiuc, R., Radu, T., Florea, A., Stiufiuc, G., Dutu, A., ... & Lucaciu, C. M. (2015). Polyethylene glycol-mediated synthesis of cubic iron oxide nanoparticles with high heating power. Nanoscale research letters, 10(1), 1-16. https://doi.org/10.1186%2Fs11671-015-1091-0

Jokerst, J. V., Lobovkina, T., Zare, R. N., & Gambhir, S. S. (2011). Nanoparticle PEGylation for imaging and therapy. Nanomedicine, 6(4), 715-728. https://doi.org/10.2217/nnm.11.19

Kurniasih, I. N., Keilitz, J., & Haag, R. (2015). Dendritic nanocarriers based on hyperbranched polymers. Chemical Society Reviews, 44(12), 4145-4164. https://doi.org/10.1039/C4CS00333K

Lane, L. A., Qian, X., Smith, A. M., & Nie, S. (2015). Physical chemistry of nanomedicine: understanding the complex behaviors of nanoparticles in vivo. Annual review of physical chemistry, 66, 521-547. https://doi.org/10.1146/annurev-physchem-040513-103718

Lazarovits, J., Chen, Y. Y., Sykes, E. A., & Chan, W. C. (2015). Nanoparticle–blood interactions: the implications on solid tumour targeting. Chemical Communications, 51(14), 2756-2767. https://doi.org/10.1039/C4CC07644C

Lee, K. Y., Wang, Y., & Nie, S. (2015). In vitro study of a pH-sensitive multifunctional doxorubicin–gold nanoparticle system: Therapeutic effect and surface enhanced Raman scattering. RSC Advances, 5(81), 65651-65659. https://doi.org/10.1039/C5RA09872F

Li, X., Takashima, M., Yuba, E., Harada, A., & Kono, K. (2014). PEGylated PAMAM dendrimer–doxorubicin conjugate-hybridized gold nanorod for combined photothermal-chemotherapy. Biomaterials, 35(24), 6576-6584. https://doi.org/10.1016/j.biomaterials.2014.04.043

Liu, L., Tang, Y., Dai, S., Kleitz, F., & Qiao, S. Z. (2016). Smart surface-enhanced Raman scattering traceable drug delivery systems. Nanoscale, 8(25), 12803-12811. https://doi.org/10.1039/C6NR03869G

Moustaoui, H., Movia, D., Dupont, N., Bouchemal, N., Casale, S., Djaker, N., ... & Spadavecchia, J. (2016). Tunable design of Gold (III)–Doxorubicin Complex–PEGylated nanocarrier. The golden doxorubicin for oncological applications. ACS applied materials & interfaces, 8(31), 19946-19957. https://doi.org/10.1021/acsami.6b07250

Rosa, S., Connolly, C., Schettino, G., Butterworth, K. T., & Prise, K. M. (2017). Biological mechanisms of gold nanoparticle radiosensitization. Cancer Nanotechnology, 8(1), 1-25. https://doi.org/10.1186/s12645-017-0026-0

Siegel, R. L., Miller, K. D., & Jemal, A. (2018). Cancer statistics, 2018. CA: A Cancer Journal for Clinicians, 68(1), 7-30. https://doi.org/10.3322/caac.21442

Tian, F., Bonnier, F., Casey, A., Shanahan, A. E., & Byrne, H. J. (2014). Surface enhanced Raman scattering with gold nanoparticles: effect of particle shape. Analytical Methods, 6(22), 9116-9123. https://doi.org/10.1039/C4AY02112F

Venkatesan, R., Pichaimani, A., Hari, K., Balasubramanian, P. K., Kulandaivel, J., & Premkumar, K. (2013). Doxorubicin conjugated gold nanorods: a sustained drug delivery carrier for improved anticancer therapy. Journal of Materials Chemistry B, 1(7), 1010-1018. https://doi.org/10.1039/C2TB00078D

Wolinsky, J. B., & Grinstaff, M. W. (2008). Therapeutic and diagnostic applications of dendrimers for cancer treatment. Advanced drug delivery reviews, 60(9), 1037-1055. https://doi.org/10.1016/j.addr.2008.02.012

Zhang, L., Zhu, S., Qian, L., Pei, Y., Qiu, Y., & Jiang, Y. (2011). RGD-modified PEG–PAMAM–DOX conjugates: In vitro and in vivo studies for glioma. European journal of pharmaceutics and biopharmaceutics, 79(2), 232-240. https://doi.org/10.1016/j.ejpb.2011.03.025

Zhang, W. L., Li, N., Huang, J., Yu, J. H., Wang, D. X., Li, Y. P., & Liu, S. Y. (2010). Gadolinium-conjugated FA-PEG-PAMAM-COOH nanoparticles as potential tumor-targeted circulation-prolonged macromolecular MRI contrast agents. Journal of applied polymer science, 118(3), 1805-1814. https://doi.org/10.1002/app.32494

Zhong, Y., Wang, C., Cheng, R., Cheng, L., Meng, F., Liu, Z., & Zhong, Z. (2014). cRGD-directed, NIR-responsive and robust AuNR/PEG–PCL hybrid nanoparticles for targeted chemotherapy of glioblastoma in vivo. Journal of Controlled Release, 195, 63-71. https://doi.org/10.1016/j.jconrel.2014.07.054

Zong, S., Wang, Z., Chen, H., Yang, J., & Cui, Y. (2013). Surface enhanced Raman scattering traceable and glutathione responsive nanocarrier for the intracellular drug delivery. Analytical chemistry, 85(4), 2223-2230. https://doi.org/10.1021/ac303028v